IJST EXPLORE International Journal of Science and Technology
CENTRE OF PROFESSIONAL RESEARCH PUBLICATIONS
ISSN 2049-7318
International Journal of Science and Technology Volume 5 No. 6, June, 2016

Effect of Magnesium Doping on the Optical and Electrical Properties of Cd-Se Quantum Dots

Ishu Sharma
Department of Physics, Amity University, Dubai, UAE.

ABSTRACT

Present study reports that Cd-Se nanoparticles with zinc blende structure allow Magnesium (Mg) Doping. Size tunable pure Cd-Se and Mg doped Cd-Se nanocrystal quantum dots were synthesized by inverse micelles technique. Paraffin oil and oleic acid were used as a solvent and surfactant respectively. Reduction in particles size with increase in Mg content is estimated from X-ray diffraction (XRD) peaks and some theoretical formulations. UV-Vis absorption spectra (300-900 nm) show a clear cut size dependent blue shift with the addition of Mg content, as a result of quantum confinement effect. The optical band gap, calculated using Tauc's plot, increases with increase in Mg doping in Cd-Se lattice. Temperature dependent electrical conductivity reveals that the dark conductivity and charge carrier concentration decreases with the addition in Mg content. The dark activation energy is calculated using Arrhenius plots. A good agreement is seen in experimentally calculated optical band gap and dark activation energy. Both are found to increase with increase in Mg content. The results show that doping of Mg significantly influence the particle size, optical band gap, activation energy and conductivity in Cd-Se quantum dots. Tailoring of optical and electrical properties in effective way, with Mg doping, control their light emission colours and maybe useful for opto-electronic devices.

Key Words: *Quantum Dots, Particle Size, Optical Gap, Dark Conductivity, Activation Energy*

1. INTRODUCTION

Confinement strongly modifies the energy spectrum of carriers. That is why quantum dots are investigated in different aspects and have potential applications [1, 2] because of their unique size dependent optical properties. However applications of quantum dots are still mostly confined to research laboratories but have remarkable applications in optics, where quantum dots are used to produce single photon and photon pairs [3, 4]. The luminescent quantum dots have excellent optical properties and higher photochemical stability than most organic emitters [5]. They have potential applications in biological imaging as fluorescent label source [6]. The core shell quantum dots are having well defined forte in the field of photonic applications such as nonlinear optical devices, solar cells, LED [7]. The quantum confinement effect appears as a blue shift in absorption, emission spectra, resulting in raise in optical gap very often [8].

Among II-VI direct band gap semiconductor nanomaterials, colloidal Cd-Se quantum dots are distinguished and most investigated for their photonic applications. They show almost full visible range light emission and have immense potential applications. They have high luminescence quantum yield, narrow band gap and variety of optoelectronic conversion properties [8-10]. With change in synthesis time and temperature, the particles size varies, which further results in change in the optical and electrical properties. In addition, doping is also one of the simple methods to tailor the properties of quantum dots. Surface morphology, shape and crystal structure of nanocrystals are important factors to determine the doping concentration in the nanocrystals. Doping wurtzite Cd-Se, commonly crystalline phase, is still limited due to self-purification. Moreover, it is proposed by Norris and co-workers [11] that when II-VI semiconductors possess zinc-blende structure i.e. (001) facets with very high binding energy only then impurities can be incorporated. As such, we prepared pure and Mg doped (0.02, 0.04 and 0.06 mole) Cd-Se quantum dots with Inverse Micelle technique using paraffin oil and oleic acid as surface capping agent. This technique is green, simple, fast and a room temperature method. Mg-Se is having higher band gap (3.60 eV) as compared to pure Cd-Se. So, it is assumed that with Mg doping, light emission wavelength can be controlled, because of assumed blue shift in absorption spectra. Present work deals with the synthesis of pure and doped Cd-Se nanocrystals with zinc blende structure, determination of optical band gap using Tauc's plot for direct band gap structures. Temperature dependent electrical measurements are also made to calculate dark conductivity, dark activation energy and charge density with different Mg content.

2. EXPERIMENTAL DETAILS

Cadmium oxide (4N pure), selenium shots (5N pure) and magnesium acetate (98% Sigma Aldrich) were used as precursors for the synthesis of Mg-Doped CdSe nanocrystals. Paraffin oil and oleic acid (Sigma Aldrich) were used as a solvent and surfactant, respectively. In step one, in a round bottom flask, 0.1 M of CdO, 25 ml of paraffin oil and 15 ml of oleic acid were mixed. The solution was heated to 160 °C and stirred properly until the CdO was completely dissolved and a homogeneous solution of light yellowish colour was obtained. In the second step, 0.02M of Se in 50 ml of paraffin oil was carefully heated to 220 °C with rapid stirring in another round bottom flask. The solution turned orange followed by wine red colour. In third step, about 5 ml of Cd

solution (maintained at 160°C) was mixed into Se solution with rapid stirring. The solution colour immediately turned into wine red and then dark brown. The temperature was maintained at 220 °C for about 40 minutes for the growth of the nanoparticles. The solution was set to cool down at room temperature. The precipitates were isolated from the solvents and unreacted reagents by centrifugation. In the last step, the precipitates were washed and cleaned with toluene several times and set to dry [12]. For synthesis of Mg-doped CdSe QDs, CdO, Se shot and magnesium were used as precursors. Paraffin oil and oleic acid were used as solvent and surfactant, respectively. Most details of the synthesis are similar as explained above. CdO and Mg acetate were added into a mixture of paraffin oil and oleic acid (25:15) by 0.1 and 0.02M, respectively. The solution was heated to 160 ^{0}C with rapid stirring. In next step, Se (0.02M) was added to 50 ml of paraffin oil in another round bottom flask. The solution was heated to 220 ^{0}C with rapid stirring till Se got completely dissolved. When solution turned orange in colour, 5 ml of Cd-Mg solution was swiftly mixed into the Se solution carefully, which allowed fast nucleation and slow growth of Mg-doped CdSe nanocrystals. The temperature was maintained at 220 ^{0}C for about 40 minutes. Then the mixture was allowed to cool down at room temperature. Precipitates were isolated with centrifuge followed by multiple wash with toluene solution and allowed to dry. The same process was repeated for 0.04 and 0.06 M Mg acetate.

For structural analysis, X-ray diffraction was carried out using a Bruker D8 Advanced diffractometer with a scanning rate of 0.02^0 s^{-1}. As-prepared nanocrystals, dispersed in toluene by sonication, were analysed for optical band gap characterization. The absorption spectra of Mg doped Cd-Se quantum dots (0, 0.02, 0.04 and 0.06 M) suspensions were measured by UV-Vis spectrophotometer (U-3010 Hitachi) in the wavelength range 300-900 nm. For electrical measurements, thin films of pure and Mg doped Cd-Se were prepared using spin coater on cleaned glass substrate. The colloidal solution was prepared using Toluene. The substrates were ultrasonically cleaned with DI water, a dip in acetone followed by ethyl alcohol and finally set to dry in oven at approximately 110 ^{0}C. Pre deposited thick indium electrodes on well cleaned gas substrate were used for electrical contacts. For the electrical measurements a suitable planar geometry of the film i.e. (length ~0.75 cm and electrode gap ~ 0.15 cm) was used. The thickness of the film was measured using the weight differential method [13]. These films were kept in the deposition chamber in the dark for about 24 hours for attaining thermodynamic equilibrium before being mounted in the metallic sample holder. The dark current was noted by digital pico-ammeter (Kitheley 6517B). A vacuum of about 10^{-3} mbar was maintained throughout these measurements.

3. RESULTS AND DISCUSSION

3.1. Structural Analysis

Figure 1 shows the X-ray diffraction pattern for Cd-Se and Mg doped (0.02 M, for reference) Cd-Se nanoparticles, which shows the formation of quantum dots with zinc-blende structure. It is clear from the figure that peaks obtained in (111), (220) and (311) planes match with zinc blende structure. The Zinc blend structure is most probably due to low synthesis temperature and complicated structure of surfactant [14]. At low temperature, it is seen that Zinc blend Cd-Se is kinetically favourable phase as well as thermodynamically metastable. The values of FWHM for Cd-Se QDs is found to be 0.098 degrees and 2.39 degrees for Mg-doped Cd-Se QDs. The particle size is calculated using the Scherrer's relation i.e. $d= (0.9\lambda)/ (\beta \cos \theta)$ [15] where β is FWHM in radians, λ is wavelength of X-rays used and θ is the Bragg's angle. From XRD pattern, it is observed that with Mg doping, particle size decreases. The particle size for Cd-Se QDs is found to be approximately 8 nm and for Mg-doped Cd-Se, is found to shrink to approximately 4 nm i.e. Mg doping results in contraction of lattice constants. This may be probably due to the smaller size of Mg^{2+} ion ($0.57A^0$) as compared to Cd^{2+} ion (0.78 A^0) in coordination number 4. Same trend is observed in ZnO thin films with Mg doping [16]. This variation of lattice constant is related to the radius difference of substitutional ion and corresponding change of the crystal structure. On comparing two XRD patterns, it was observed that XRD peak intensity in case of Mg-doped Cd-Se QDs is decreasing as compared to the intensity of pure Cd-Se QDs. Though, no noticeable peak shift is observed with Mg doping. So, it is assumed that Mg^{2+} ions, relatively small in size, firstly occupy empty interstitial sites of Cd-Se instead of filling substitutional sites of Cd^{2+}.

3.2. UV-Vis absorption spectra

Figure 2(a) shows the absorption spectra of pure and Mg doped Cd-Se (Mg = 0.02, 0.04 and 0.06 mole) quantum dots. From the figure, it is observed that Cd-Se nano crystallites are tunable with the Mg doping. High absorption peaks are observed in short wavelength range for all the samples. A gradual blue shift is observed in excitonic peak with the addition of Mg in Cd-Se quantum dots. Also, it is found that, size of doped QDs goes on decreasing with increase of Mg content. This size difference may presumably be the reason for observed blue shift. Though not calculated, but it can be qualitatively shown that with the addition of Mg content, refractive index of the quantum dots decreases. This decrease in refractive index may be due to the smaller polarizability (due to the smaller size of Mg^{2+} ion as compared to Cd^{2+}). It has been reported that in the zinc blend unit cell, Mg^{2+} ions partially fulfil the tetrahedral interstitial sites, in which 4 out of 8 sited are occupied by Cd^{2+} ion [17]. Smaller the atomic radius of atom, smaller will be the polarizability and according to Lorentz–Lorentz relation,

$\frac{n^2-1}{n^2+2} = \frac{1}{3\epsilon_0}\sum_i N_i \alpha_{pi}$ smaller will be the refractive index. Moreover, from the Kramer-Kronig relation, $n(o) - 1 = \left(1/2\pi^2\right)\int_0^\infty \alpha d\lambda$, as experimentally obtained, blue shift in absorption spectrum, must necessarily give a decrease in refractive index values. The decrease in refractive index, with increase in Mg, may also be because of addition of lighter Mg (1.738 g/cc at RT) as compared to Cd (8.65 g/cc at RT), and hence with the decrease in density, refractive index value falls.

3.2.1. The determination of the absorption coefficient and optical band gap

The absorption peaks are used to estimate the change in optical band gap with the increase in Mg content. The absorption coefficient 'α' of pure and Mg-doped Cd-Se is calculated using Beer Lambert's relation, $\alpha = 2.303(x/d)$, where '*x*' is the absorbance and *d* is the path length of quartz cuvette. The optical band gap is calculated, for this commonly accepted "direct transition", from Tauc's relation using absorption coefficient, $(\alpha h\nu)^2 = B^2(h\nu - E_g^{opt})$, where, $h\nu$ is the energy of photon, α is the absorption coefficient, E_g^{opt} optical band gap and B^2 represents Tauc slope. In crystalline materials, the density of states lies in band separated by energy gaps, as a consequence of defects [18]. The Tauc relation assumes that the density of the electron states will have a parabolic distribution and for the inter-band transitions, the matrix elements associated with the photon absorption will be equal for all the transitions. Figure 2(b) shows the variation of $(\alpha h\nu)^2$ with $h\nu$. By extrapolating the best line between $(\alpha h\nu)^2$ and $h\nu$, to intercept $h\nu$ axis $(\alpha = 0)$ the band gap is calculated. Table 2 summarizes the variation of band gap with Mg doping and it increases from 2.1 to 3.6 eV with doping. The bandgap of Cd-Se quantum dot (2.1 eV) is found to be larger than that of bulk Cd-Se (1.74 eV). This indicates that with the decrease in particle size, the absorption spectra shift towards lower wavelength. It is reflected from tabulated values that Mg addition induces structural modification in the host matrix. Mg atom substitution into Cd-Se lattice reduces the defects. It may enter into interstitial sites of host network and vacancy defects could be depressed as discussed earlier. This reduction in defect, (some of the crystalline defects that is stacking faults may be assumed to be present during crystal growth) may also account for increase in optical band-gap with the addition of Mg. It is observed that inner band defect states are also present between conduction band and valence band, and the dopants (activators) perturb the inner band structure [19, 20]. The width of these states reduces with the lessening of defects, and further results in the increase in optical gap. Moreover, because of low electronegativity value of magnesium, the Mg dopants contribute more electrons as compared to Cd. This increase in contribution takes up the energy level of conduction band [16]. This results in an increase in band gap values or observed shift of absorption edge, towards lower wavelength region, with the increase in Mg.

3.3. Temperature dependent electrical conductivity

For Mg doped Cd-Se (Mg = 0.02, 0.04 and 0.06 mole) quantum dots thin films, the temperature dependent dark conductivity (σ_d) measurements were taken at room temp (303 K) and are shown in figure 3. $\ln\sigma_d$ vs 1000/T plot is straight line for all the samples under observation. These straight lines clearly indicate that the conduction is through an activated process, having single activation energy in the temperature range 303–360 K. In most of the chalcogenide glasses, σ_d can be expressed by the following Arrhenius relation [21] $\sigma_d = \sigma_0 \exp\left(\frac{-\Delta E_d}{kT}\right)$ where, σ_0 represents the material-related pre-exponential factor, ΔE_d represents the activation energy for dc conduction, *k* is the Boltzmann's constant and *T* is temperature. From the slope of $\ln\sigma_d$ versus 1000/T curves, the values of dark activation energy (ΔE_d) are calculated. The values of σ_0 are calculated by substituting the values of ΔE_d and σ_d in above equation at 303K. The values of ΔE_d and σ_d are tabulated in table 2 along with pre-exponential factor (σ_0). It is observed that, with the increase in Mg content, the dark activation energy increases and an appreciable decrease is found in electrical conductivity, for all the samples at room temperature. This indicates that the Mg doping concentration, defects (interstitial, vacancies) and scattering centres accounts for the change in electrical parameters. The value of carrier concentration also influences the conductivity. Charge carrier density is calculated using $n_\sigma = 2\left(\frac{2\pi mkT}{h^2}\right)^{\frac{3}{2}} \exp\left(\frac{-\Delta E_d}{kT}\right)$ where '*m*' is the charge carrier's mass and '*k*' is the Boltzmann's Constant and are tabulated in table 2. It is observed that the density of charge carriers decreases with the addition of Mg which may further account for the decrease in conductivity. After doping, Mg may form bond with Se, leaving behind voids. These voids may trap free carriers, results in decrease in charge carrier concentration and defects, and consequently contributes towards decrease in conductivity. This is also responsible for the increase in the activation energy. Same trend is observed in the behaviour of optical gap with increasing Mg concentration. This change may be because of wide band gap value of MgSe (3.60 eV) as compared to CdSe (1.74 eV). This Mg doping might change the acceptor/ donor concentration and therefore results in change in resistivity/ conductivity and may be attributed to the quantum confinement effect or decrease in size of quantum dot with Mg doping.

3.4. Correlation between particle size and optical gap

The calculated size of quantum dots is summarized in table 2. From the tabulated values, it is clear that the particle size is less than the Bohr radius, and hence the prepared nanoparticles are well with the quantum confinement. It is found that the band gap of nanoparticles is closely related to their optical band gaps. On the basis of quantum confinement theory [22,23], the size of the quantum dots is estimated using the calculated band gap values using Brus-equation, $E_g(dot) = E_g(bulk) + \frac{h^2}{8r^2}\left[\frac{1}{m_e^*} + \frac{1}{m_h^*}\right] - \frac{1.8e^2}{4\pi\varepsilon_0\varepsilon_r r}$, where $E_g(dot)$ is the band gap of quantum dots, calculated experimentally, using Tauc's plot (table 2) for pure and doped CdSe. The band gap energy of their bulk counterparts are $E_g(bulk)$ = 1.74eV for CdSe and 1.92 eV for Mg doped CdSe [17]. Where '*h*' is the Planks constant, '*r*' is the radius of the particle. Also $m_e^* = m_e m_0 = 0.12 m_0$ and $m_h^* = m_h m_0 = 0.8 m_0$, where m_0 is the mass of electron, ε_r represents relative dielectric constant and ε_0 is space dielectric constant [24] . According to some researchers, the above Brus effective mass approximation model, used to calculate particle size is considered to be quite rough [25]. According to this model the QDs are assumed to be spherical and that the effective mass of the charge carriers and dielectric constant of the solids are constant as a function of size. So two empirical equations have been proposed by Yu *et al* and Bacherikov *et al* [26, 27], $D = (1.6122x10^{-9})\lambda^4 - (2.6575x10^{-6})\lambda^3 + (1.6242x10^{-3})\lambda^2 - (0.4277)\lambda + (41.57)$ …(A) and $D = 0.344e^{(\lambda - 252.7)/129.3}$ …(B), where, $\lambda(nm)$ is the wavelength corresponding to first excitonic absorption peak. It is observed that with the addition of Mg to Cd-Se, the particle size decreases. Same results are confirmed from XRD plots also. From the table it is clear that, decrease in size leads to increase in optical gap, which reflects blue shift of absorption spectra**.**

4. CONCLUSION

The inverse micelle technique is used for the synthesis of pure and Mg doped (0.02, 0.04 and 0.06) Cd-Se quantum dots. Study of the XRD peaks reveals the formation of zinc blende structure. Particles size, as estimated from XRD peaks and some theoretical formulations, is found to decrease with the increase in Mg content. It is also observed that the particle size is less than 10 nm in all cases. Mg doping facilitates the tailoring of Cd-Se quantum dots for specific applications. Absorption spectra show blue shift with doping attributes enhanced optical properties. Raise in band gap values shows quantum confinement effect. The optical gap increases with the reduction in particle size. The electrical measurements (at room temperature) exhibit decrease in the charge carrier concentration with increase in Mg doping and further accounts for the decrease in the electrical conductivity. Mg doping may reduce the disorder in the system and hence results in reduction of width of tail states which are further reflected in the pattern of dark activation energy. ΔE_d values increase with the increase in Mg content. Moreover, the present study details the green synthesis of Mg doped Cd-Se QDs using inverse micelle technique and shows the possibility of doping in the Zinc blende structure. Hence this technique can be further explored for easy synthesis of other tunable nanomaterials.

Acknowledgement

Author is grateful to Dr A.K. Shukla and Ms Neha Bhardwaj from Amity University, Noida for their contribution in carrying out experimental part and also thankful to Amity University, Noida, U.P for providing every required lab facility.

REFERENCES

Kim, D.G., Teratani, N. and Nakayama, M. (2002). Self-Narrowing and Photoetching Effects on the Size Distribution of CdS Quantum Dots Prepared by a Reverse-Micelle Method. Jpn. J. Appl. Phys., 41: 5064-5068.

Pradhan, N., Goorskey, D., Thessing, J., and X Peng. (2005). An Alternative of CdSe Nanocrystal Emitters: Pure and Tunable Impurity Emissions in ZnSe Nanocrystals. J. Am. Chem. Soc. 127: 17586-87.

Michler, P., Imamoglu, A., Mason. M.D., Carson, P.J., Strouse, G.F. and Buratto, S.K. (2000). Quantum correlation among photons from a single quantum dot at room temperature. Nature, 406: 968-970.

Akopian, N., Lindner, N.H., Poem, E., Berlatzky, Y., Avron, J., Gershoni, D., Gerardot, B.D. and Petro, P.M. (2006). Entangled photon pairs from semiconductor quantum dots. Physical Review Letters, 96(13): 130501-130504.

Ishizumi, A. and Kanemitsu, Y. (2006). Luminescence Spectra and Dynamics of Mn-Doped CdS Core/Shell Nanocrystals. Adv. Mater., 18(8): 1083-1085.

Bailey, R.E., Smith, A.M. and Nie, S. (2004). Quantum dots in biology and medicine. Physica E, 25: 1-12.

Mathew, S. and Saran, A.D. (2012). Size dependent optical properties of the CdSe-CdS core-shell quantum dots in the strong confinement regime. Journal of Applied Physics, 111(7): 074312/1-074312/8.

Wen, Mi., Tian, J., Tian, W., Dai. J., Wang, X. and Liu, X. (2012). Temperature dependent synthesis and optical properties of CdSe quantum dots. Ceramics International, 38: 5575-5583.

Bruchez, M.J., Moronne, M., Gin, P., Weiss, S. and Alivisatos, A.P. (1998) Semiconductor Nanocrystals as Fluorescent Biological Labels. Science, 281: 2013-2016.

Zhu, J.J., Palchik, O., Chen, S. and Gedanken, A. (2000). Microwave Assisted Preparation of CdSe, PbSe, and $Cu_{2-x}Se$ Nanoparticles. J. Phys. Chem. B., 104(31):7344-7347.

Erwin, S.C., Zu, L.J., Haftel, M.I., Efros, A.L., Kennedy, T.A., Norris, D.J. (2005). Doping semiconductor nanocrystals. Nature, 436: 91-94.

Hamizi, N.A. and Johan, M.R. (2010). Synthesis and size dependent optical studies in CdSe quantum dots via inverse micelle technique, Materials Chemistry and Physics. 124: 395- 398.

Choi, J.Y, Kim, K.J., Yoo, B.J. and Kim, D. (1998). Properties of cadmium sulfide thin films deposited by chemical bath deposition with ultrasonication. Solar Energy, 64 (1–3): 41–47.

Jun, Y.W., Choi, J.S. and Angew, C.J. (2006). Shape control of semiconductor and metal oxide nanocrystals through nonhydrolytic colloidal routes. Chem Int Ed Engl., 45(21): 3414-39.

Raman, S.G, Ratnam, P.S.K, Chidambaradhanu. (2010). Studies of CdSe nanoparticles synthesized by solvo-thermal route. Recent Research in Science and Technology, 2(10):72-76.

Kaushal, A. and Kaur, D. (2009). Effect of Mg content on structural, electrical and optical properties of $Zn_{1-x}Mg_xO$ nanocomposite thin films. Solar Energy Materials & Solar Cells, 93:193-198.

Kwak, W.C., Kim, T.G., Chae, W.S., Sung, Y.M. (2007). Tuning the energy bandgap of CdSe nanocrystals via Mg doping. Nanotechnology, 18: 205702-205706.

Dunstan, D.J. (1982). Evidence for a common origin of the Urbach tails in amorphous and crystalline semiconductors. Phys. C: Solid State Phys., J15: L419-424.

Bera, D., Qian, L., Tseng, T.K, Holloway, P.H. (2010). Quantum Dots and Their Multimodal Applications: A Review. Materials, 3: 2260-2345.

Issac, A., von Borczyskowski, C., Cichos, F. (2005). Correlation between photoluminescence intermittency of CdSe quantum dots and self-trapped states in dielectric media. Phys. Rev. B, 71: 161302 R(1)-R(4).

Mott, N.F and Davis, E.A. (1971). Electronics Process in Non-Crystalline Materials. Oxford: Clarendon.

Brus, L. (1986). Zero-dimensional "excitons" in semiconductor clusters. IEEE J. Quantum Electron, 22(9): 1909–1914.

Brus, L.E. (1984). Electron–electron and electron–hole interactions in small semiconductor crystallites: the size dependence of the lowest excited electronic state. Journal of Chemical Physics, 80: 4403–4409.

Berger, L.I. (1997) Semiconductor Materials. CRC Press; Boca Raton; FL.

Hendry. E., Koeberg. M., Wang, F., Zhang, H., Donega, C.M., Vanmaekelbergh, D., Bonn, M. (2006). Direct observation of electron-to-hole energy transfer in CdSe quantum dots. Physical Review Letters, 96: 057408/1-057408/4.

Yu, W.W, Qu, L., Guo, W. and Peng, X.G. (2003) Experimental determination of the extinction coefficient of CdTe, CdSe, and CdS nanocrystals. Chemistry of Materials,15: 2854–2860.

Bacherikov, Y., Davydenko, M.O., Dmytruk, A.M., Dmitruk, I.M., Lytvyn, P.M., Prokopenko, I.V., Romanyuk, R. (2006) CdSe nanoparticles grown with different chelates. Semiconductor Physics, Quantum Electronics and optoelectronics, 9: 75-79.

Table 1 XRD Position of peaks for Cd-Se and Mg doped (0.02 mole) Cd-Se

Quantum Dots	2Θ(degree)		
	Peak 1(111)	Peak 2(220)	Peak 3(311)
CdSe	25.44	41.96	49.64
Mg-doped CdSe	25.38	41.82	49.62

Table 2 Optical band gap (E_g^{opt}), diameter (d in nm) of particle obtained from Brus equation, diameter (nm) obtained from two empirical equations A and B, temperature dependent dark conductivity (σ_d) in $\Omega^{-1}\,cm^{-1}$, material-related pre-exponential factor (σ_0) in $\Omega^{-1}\,cm^{-1}$, dark activation energy (ΔE_d) in eV and charge carrier density (n_σ) in m^{-3} for pure and Mg doped Cd-Se (0.02, 0.04 and 0.06 mole).

QDs	E_g^{opt} (eV)	d (Brus) (nm)	D (empirical eq^n) (nm)	σ_d ($\Omega^{-1}\,cm^{-1}$)	σ_0 ($\Omega^{-1}\,cm^{-1}$)	ΔE_d (eV)	n_σ (m^{-3})
CdSe	2.1	2.81	A= 8.95 B= 7.36	$2.7*10^{-5}$	$1.76*10^{15}$	1.21	$1.98*10^{5}$
CdSe-Mg (0.02)	2.31	2.72	A=4.76 B=5.20	$5.5*10^{-6}$	$1.12*10^{16}$	1.28	$1.36*10^{4}$
CdSe-Mg (0.04)	3.05	1.67	A= 3.82 B= 4.32	$1.3*10^{-7}$	$3.85*10^{16}$	1.41	$0.93*10^{2}$
CdSe-Mg (0.06)	3.6	1.39	A= 3.38 B= 3.85	$5.5*10^{-7}$	$2.80*10^{19}$	1.53	1.09

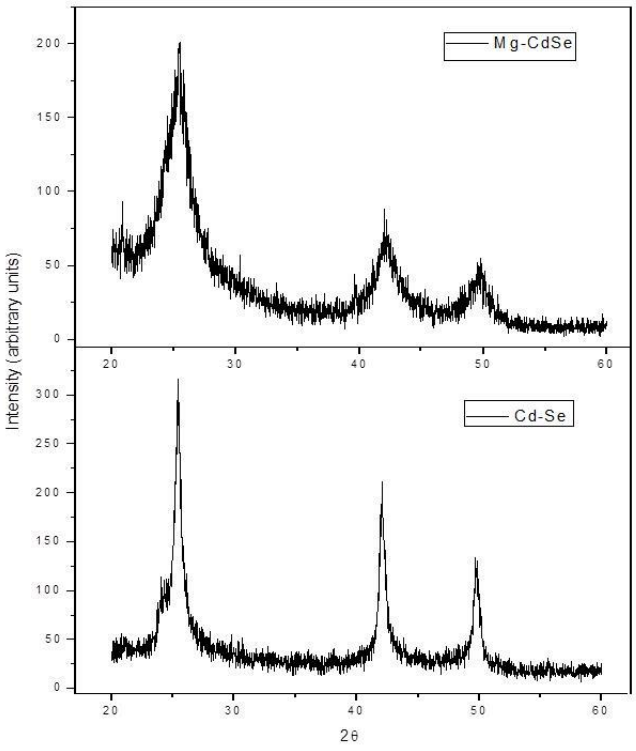

Figure 1 XRD patterns of Cd-Se and Mg-doped (0.02 mole) Cd-Se QDs.

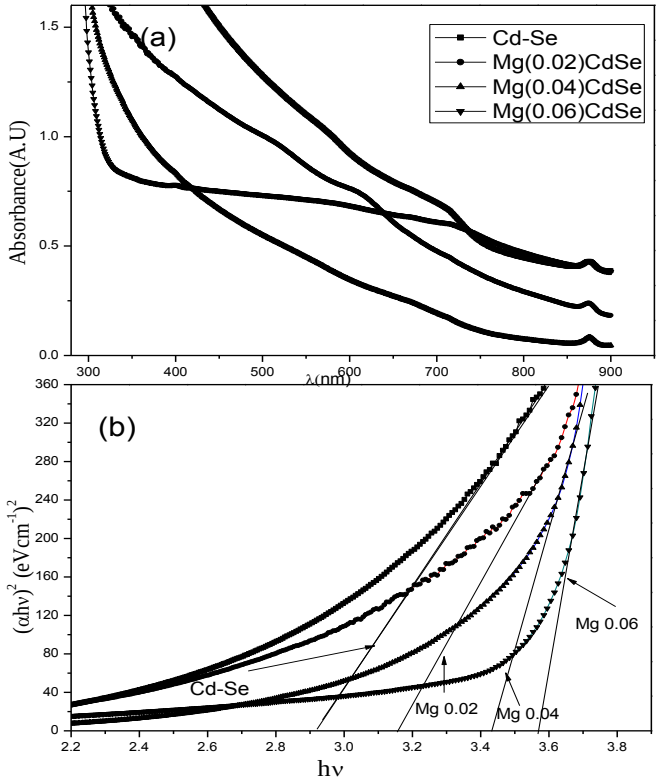

Figure 2(a) Plot of absorbance versus wavelength (nm), (b) Plot of $(\alpha h\upsilon)^2$ vs $h\upsilon$ for pure and Mg doped Cd-Se (0.02, 0.04 and 0.06 mole).

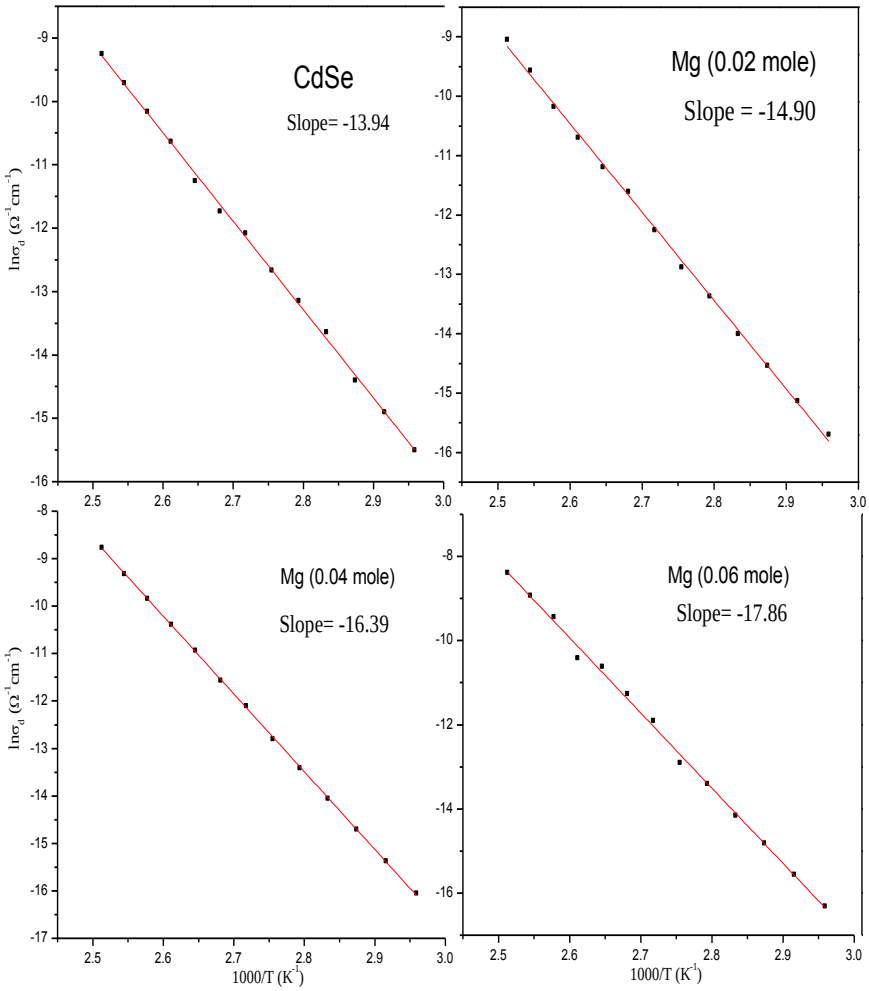

Figure 3 Temperature dependence of dark conductivity for pure and Mg doped Cd-Se (0.02, 0.04 and 0.06 mole).